LETTER

doi:10.1038/nature12400

A rigid and weathered ice shell on Titan

D. Hemingway[1], F. Nimmo[1], H. Zebker[2] & L. Iess[3]

Several lines of evidence suggest that Saturn's largest moon, Titan, has a global subsurface ocean beneath an outer ice shell 50 to 200 kilometres thick[1–4]. If convection[5,6] is occurring, the rigid portion of the shell is expected to be thin; similarly, a weak, isostatically compensated shell has been proposed[7,8] to explain the observed topography. Here we report a strong inverse correlation between gravity[3] and topography[9] at long wavelengths that are not dominated by tides and rotation. We argue that negative gravity anomalies (mass deficits) produced by crustal thickening at the base of the ice shell overwhelm positive gravity anomalies (mass excesses) produced by the small surface topography, giving rise to this inverse correlation. We show that this situation requires a substantially rigid ice shell with an elastic thickness exceeding 40 kilometres, and hundreds of metres of surface erosion and deposition, consistent with recent estimates from local features[10,11]. Our results are therefore not compatible with a geologically active, low-rigidity ice shell. After extrapolating to wavelengths that are controlled by tides and rotation, we suggest that Titan's moment of inertia may be even higher (that is, Titan may be even less centrally condensed) than is currently thought[12].

Three solutions for Titan's low-order gravity field[3,12] have been obtained via radio tracking of the Cassini spacecraft, with good constraints up to spherical harmonic degree 3. Topography data have been obtained through a combination of radar altimetry and analysis of the overlapping portions of Cassini radar images[13]. Spherical harmonic models[9,14] have been generated to represent the topography globally. Because of data gaps, the coefficients derived can depend on the maximum degree allowed for the harmonic expansion, but are stable up to degree 6 (Supplementary Information).

The degree-3 signal is useful because, although it is small compared to those at degrees 2 and 4, it is not directly affected by tides, rotation or tidal heating[7]. Figure 1 illustrates the negative correlation between the degree-3 gravity (Fig. 1a) and topography (Fig. 1b) signals for one set of gravity and topography data. We employ an admittance analysis[15,16], which measures the gravity-to-topography ratio in a way that is not biased by uncorrelated signals in the gravity data (Supplementary Information). For example, there may be gravity anomalies sourced from the deeper interior, but they should not show a strong correlation with surface topography. The degree-3 admittance appears to be substantially negative, and a Monte Carlo analysis shows that this result is robust to the estimated uncertainties (Fig. 2).

Negative admittances are rare. They can occur in convecting systems with strong viscosity stratification[17], but it is unclear why Titan's ice shell would have such layering, and the shell is sufficiently thin that—as for Enceladus[18]—convective features should have much shorter horizontal length scales than degree 3.

Titan's long-wavelength surface topography probably arises from small (~1%) variations in shell thickness[7], which may be related to tidal heating (Supplementary Information). Such variations in shell thickness can give rise to negative admittances only if the shell is rigid and loading occurs primarily from below, leading to roots at the base of the ice shell that are large compared with the isostatic case (Supplementary Information). Here we model this situation, taking into account loading from both the top (for example, sedimentation or erosion at the surface) and bottom (for example, freezing or melting at the base of the ice shell), and calculate the resulting deformation using the equations of flexure on a thin elastic shell[19–21].

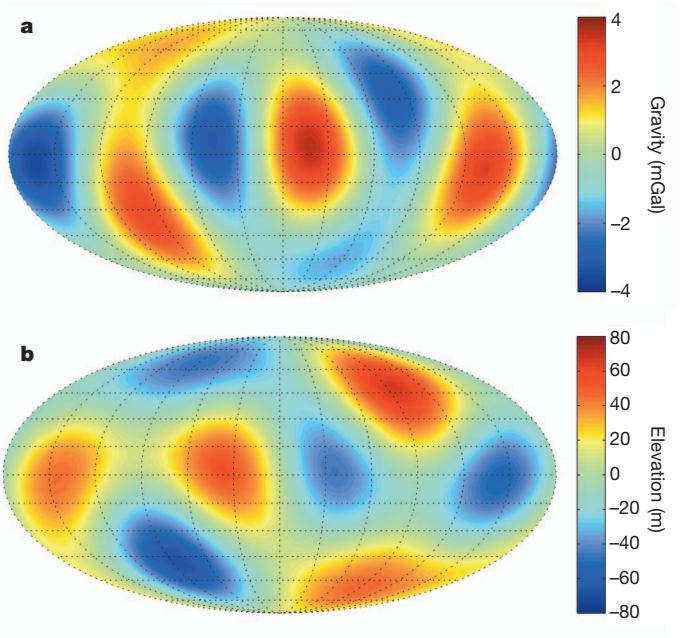

Figure 1 | Titan's degree-3 gravity and topography. **a**, Gravity field derived from the potential coefficients of the SOL1a gravity field representation of ref. 3 (multi-arc analysis, 3 × 3 gravity field). **b**, Spherically referenced topography based on degree-6 harmonic expansion[9] (Supplementary Information). The two signals display a strong negative correlation (with correlation coefficient $\gamma = -0.61$) and give rise to an admittance of –32 mGal km^{-1}, based on a Monte Carlo analysis accounting for the uncertainty in the two signals (Supplementary Information). Maps are shown in Mollweide projection, centred on the anti-Saturnian point (180° longitude).

If the observed surface topography h and the amount of top loading d_t are specified, and if top and bottom loads are in phase, it can be shown (Supplementary Information) that the degree-l admittance is given by

$$Z(l) = \frac{l+1}{2l+1} 4\pi G \rho_{\mathrm{crust}} \left[1 - \left(\frac{1 - \frac{d_t}{h}}{C} + \frac{d_t}{h} \right) \left(1 - \frac{d}{R} \right)^{l} \right] \qquad (1)$$

where d is the mean ice-shell thickness, R is Titan's mean radius and ρ_{crust} is the crustal (that is, ice shell) density. The quantity d_t is the amount of material added or subtracted at the top of the shell: negative values of d_t indicate removal of material (erosion) from pre-existing highs and deposition at lows. Here C is the compensation factor at degree l; when $C = 1$, the topography is fully compensated (isostatic) and admittance is necessarily positive. When $C < 1$, the load is partly

[1]Department of Earth and Planetary Sciences, University of California Santa Cruz, 1156 High Street, Santa Cruz, California 95064, USA. [2]Departments of Geophysics and Electrical Engineering, Stanford University, Stanford, California 94305, USA. [3]Dipartimento di Ingegneria Meccanica e Aerospaziale, Università La Sapienza, 00184 Rome, Italy.

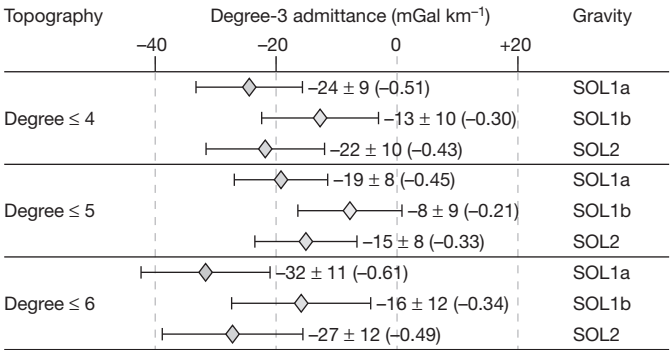

Figure 2 | Admittance estimates for nine sets of gravity and topography data. Three distinct gravity models[3] and three distinct topography models[9] (truncated at harmonic degrees 4, 5 and 6) were used to produce a total of nine separate admittance estimates. Each estimate is based on a Monte Carlo analysis in which the admittance was computed for each of 100,000 distinct sets of gravity and topography coefficients, distributed according to the 1σ uncertainties in the model coefficients. For each Monte Carlo analysis, diamonds are plotted at the mean admittance estimate, and 1σ error bars are shown to represent the distribution. To the right of the error bars are the mean ± standard deviation of the admittance estimates in milligals per kilometre, followed by the correlation coefficients γ in parentheses.

supported by elastic flexure of the ice shell and admittance may be negative for sufficiently small values of C or sufficiently negative values of d_t/h. In the case of degree 3, and assuming reasonable ice-shell properties (Supplementary Information), C is so large that admittance cannot be negative unless d_t/h is negative (that is, when erosion has occurred in areas of positive topography).

The black line plotted in Fig. 3a indicates the admittance corresponding to Fig. 1 and shows that more than 100 m of surface erosion is required even for very large (~400 km) elastic thicknesses. If the elastic thickness is less than 40 km, more than ~1 km of erosion is required. Figure 3b plots combinations of d, T and d_t that satisfy the observed admittance. For an ice-shell thickness of 200 km, for example, more than 200 m of erosion are required. As the elastic layer decreases in thickness, there is an increase in both the implied amount of erosion, and the absolute uncertainty in that estimate (Supplementary Information). Using $Z(3) = -32 \pm 11$ mGal km^{-1}, the uncertainty in the admittance estimate produces approximately ±30% uncertainty in the erosion estimate (where one galileo is defined as one centimetre per second squared).

The survival of large-impact basin rims and other topographic features[10,11] rules out erosion amplitudes greater than ~1 km, implying a shell elastic thickness greater than 40 km (Fig. 3b). This high rigidity could be the result of a cold (ammonia-rich) subsurface ocean[22,23], a clathrate-rich shell[4] or a low heat flux from the interior (Supplementary Information). The addition of a rigid shell would slightly reduce the k_2 tidal Love number, but not enough to conflict with the measured value[3] (Supplementary Information). The implied elastic thickness rules out a vigorously convecting shell, limits the potential for widespread cryovolcanism[22,24], and permits the survival of lateral shell thickness variations (Supplementary Information). To generate the observed topography, our model requires shell thickness variations at degree 3; possible sources include tidal heating in a laterally heterogeneous shell[25], and redistribution of material via non-Newtonian lateral flow[26] (Supplementary Information). A rigid conductive shell is also only weakly dissipative, potentially helping to explain Titan's high present-day orbital eccentricity[4,7].

Our lower bound on the extent of erosion and deposition (200 m) over global length scales is compatible with estimated local amounts based on impact crater degradation[10,11], but somewhat larger than estimates from fluvial incision[27]. The implied vertical erosion/deposition rate is of the order of a metre per million years, comparable to the lower end of aeolian deposition rates measured on Earth[28]; erosion may be

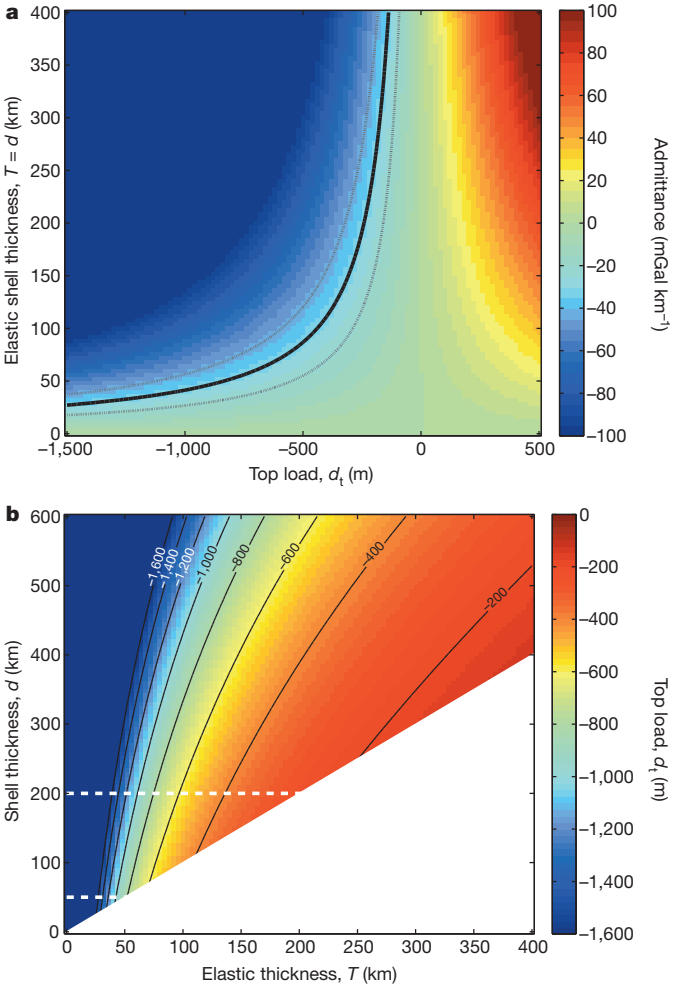

Figure 3 | Model predictions of admittance and erosion. **a**, Degree-3 admittance predicted by our model for various combinations of elastic thickness T and top load d_t, here assuming that T equals the shell thickness d. Larger values of T correspond to smaller values of C (that is, less compensation). Negative top load indicates erosion at topographic highs and deposition at topographic lows. The solid black line indicates the admittance corresponding to Fig. 1 (−32 mGal km^{-1}); the dashed lines indicate the 1σ uncertainty on that estimate. Whereas the rheology of ice implies that $T \approx 0.5d$ (Supplementary Information), assuming that $T = d$ leads to conservative estimates of erosion. **b**, Top load amplitude, d_t, required to produce the observed degree-3 admittance for various combinations of total shell thickness d and elastic thickness T. Dashed white lines highlight the likely range of Titan's ice shell thickness, 50–200 km. Both **a** and **b** were generated assuming a degree-3 topographic amplitude h of 66 m.

occurring by physical comminution, dissolution or sublimation. Because Titan's topography is high at the equator, we predict maximum erosion occurring at the equator and sediment transport, via fluvial or aeolian processes, predominantly towards the poles. An alternative possibility is transport in the vapour phase, if the mobile material has a sublimation temperature close to that of the surface temperature.

The degree-2 gravity signal is dominated by tides and rotation, and has been used to determine Titan's moment of inertia[12]. If the processes identified here are also operating at degree 2, then the measured degree-2 gravity signal is an underestimate of that caused by tides and rotation (Supplementary Information). As a result, Titan's fluid Love number may be larger than the value estimated directly from the observed gravity field, indicating that Titan may be even less centrally condensed than previously thought (Supplementary Information). This result reinforces the need to understand how so large a body could have accreted without undergoing more complete differentiation[12,29].

If the ice shell is sufficiently rigid (that is, the elastic layer exceeds half of the total shell thickness), then the admittance at degree 4 should also be negative. Assuming a fully elastic shell (that is, $T = d$) of thickness 200 km, we predict the degree-4 gravity field amplitude and the degree-4 admittance to be 1.4 mGal and -5 mGal km^{-1}, respectively (Supplementary Information). Future Cassini gravity fly-bys will improve the determination of the degree-4 gravity field by a factor of two and will therefore provide a partial test of this prediction. If a non-negative degree-4 admittance is observed, that may be an indication that a smaller portion (less than half) of the ice shell is elastic.

Received 8 May; accepted 20 June 2013.

1. Béghin, C., Sotin, C. & Hamelin, M. Titan's native ocean revealed beneath some 45 km of ice by a Schumann-like resonance. *C. R. Geosci.* **342,** 425–433 (2010).
2. Bills, B. G. & Nimmo, F. Rotational dynamics and internal structure of Titan. *Icarus* **214,** 351–355 (2011).
3. Iess, L. *et al.* The tides of Titan. *Science* **337,** 457–459 (2012).
4. Tobie, G., Lunine, J. I. & Sotin, C. Episodic outgassing as the origin of atmospheric methane on Titan. *Nature* **440,** 61–64 (2006).
5. Mitri, G. & Showman, A. P. Thermal convection in ice-I shells of Titan and Enceladus. *Icarus* **193,** 387–396 (2008).
6. Tobie, G., Grasset, O., Lunine, J. I., Mocquet, A. & Sotin, C. Titan's internal structure inferred from a coupled thermal-orbital model. *Icarus* **175,** 496–502 (2005).
7. Nimmo, F. & Bills, B. G. Shell thickness variations and the long-wavelength topography of Titan. *Icarus* **208,** 896–904 (2010).
8. Choukroun, M. & Sotin, C. Is Titan's shape caused by its meteorology and carbon cycle? *Geophys. Res. Lett.* **39,** 1–5 (2012).
9. Zebker, H. A. *et al.* Titan's figure fatter, flatter than its gravity field. *AGU Fall Meet.* abstr. P23F–01 (2012).
10. Neish, C. D. *et al.* Crater topography on Titan: implications for landscape evolution. *Icarus* **223,** 82–90 (2013).
11. Moore, J. M., Howard, A. D. & Schenk, P. M. Bedrock denudation on Titan: estimates of vertical extent and lateral debris dispersion. *Lunar Planet. Sci. Conf.* **XXXXIIII,** abstr. 1763 (2013).
12. Iess, L. *et al.* Gravity field, shape, and moment of inertia of Titan. *Science* **327,** 1367–1369 (2010).
13. Stiles, B. W. *et al.* Determining Titan surface topography from Cassini SAR data. *Icarus* **202,** 584–598 (2009).
14. Zebker, H. *et al.* Size and shape of Saturn's moon Titan. *Science* **324,** 921–923 (2009).
15. McKenzie, D. The relationship between topography and gravity on Earth and Venus. *Icarus* **112,** 55–88 (1994).
16. Wieczorek, M. A. Gravity and topography of the terrestrial planets. *Treat. Geophys.* **10,** 165–206 (2007).
17. Richards, M. A. & Hager, B. H. Geoid anomalies in a dynamic Earth. *J. Geophys. Res.* **89,** 5987–6002 (1984).
18. Roberts, J. H. & Nimmo, F. Tidal heating and the long-term stability of a subsurface ocean on Enceladus. *Icarus* **194,** 675–689 (2008).
19. Kraus, H. *Thin Elastic Shells* (Wiley, 1967).
20. Turcotte, D. L., Willemann, R. J., Haxby, W. F. & Norberry, J. Role of membrane stresses in the support of planetary topography. *J. Geophys. Res.* **86,** 3951–3959 (1981).
21. McGovern, P. J. *et al.* Localized gravity/topography admittance and correlation spectra on Mars: implications for regional and global evolution. *J. Geophys. Res.* **107,** 5136 (2002).
22. Moore, J. M. & Pappalardo, R. T. Titan: an exogenic world? *Icarus* **212,** 790–806 (2011).
23. Grasset, O., Sotin, C. & Deschamps, F. On the internal structure and dynamics of Titan. *Planet. Space Sci.* **48,** 617–636 (2000).
24. Lopes, R. M. C. *et al.* Cryovolcanic features on Titan's surface as revealed by the Cassini Titan Radar Mapper. *Icarus* **186,** 395–412 (2007).
25. Běhounková, M., Tobie, G., Choblet, G. & Čadek, O. Tidally-induced melting events as the origin of south-pole activity on Enceladus. *Icarus* **219,** 655–664 (2012).
26. Nimmo, F. Non-Newtonian topographic relaxation on Europa. *Icarus* **168,** 205–208 (2004).
27. Black, B. A., Perron, J. T., Burr, D. M. & Drummond, S. A. Estimating erosional exhumation on Titan from drainage network morphology. *J. Geophys. Res.* **117,** E08006 (2012).
28. Patterson, D. B., Farley, K. A. & Norman, M. D. He-4 as a tracer of continental dust: a 1.9 million year record of aeolian flux to the west equatorial Pacific Ocean. *Geochim. Cosmochim. Acta* **63,** 615–625 (1999).
29. O'Rourke, J. G. & Stevenson, D. J. Stability of ice/rock mixtures with applications to Titan. *Lunar Planet. Sci. Conf.* **XXXXII,** abstr. 1629 (2011).

Supplementary Information is available in the online version of the paper.

Acknowledgements We thank the Cassini radar science team, M. Manga, D. Stevenson, R. Pappalardo and W. McKinnon for their suggestions. Portions of this work were supported by NASA grants NNX13AG02G and NNX11AK44G.

Author Contributions F.N. initiated the effort. D.H. and F.N. developed the loading models and analysed the results. L.I. led the development of the gravity field models. H.Z. synthesized the topography models. All authors discussed the results and implications and commented on the manuscript.

Author Information Reprints and permissions information is available at www.nature.com/reprints. The authors declare no competing financial interests. Readers are welcome to comment on the online version of the paper. Correspondence and requests for materials should be addressed to D.H. (djheming@ucsc.edu).